FILE COPY
NO 4

CONFIDENTIAL

Copy No. 267
RM No. L7E26

NACA

RESEARCH MEMORANDUM

FLIGHT TESTS TO DETERMINE THE EFFECT OF TAPER ON THE ZERO-LIFT DRAG OF WINGS AT LOW SUPERSONIC SPEEDS

By

Sidney R. Alexander and Robert L. Nelson

Langley Memorial Aeronautical Laboratory
Langley Field, Va.

THIS DOCUMENT ON LOAN FROM THE FILES OF
NATIONAL ADVISORY COMMITTEE FOR AERONAUTICS
LANGLEY AERONAUTICAL LABORATORY
LANGLEY FIELD, HAMPTON, VIRGINIA

RETURN TO THE ABOVE ADDRESS.

REQUESTS FOR PUBLICATIONS SHOULD BE ADDRESSED AS FOLLOWS:

NATIONAL ADVISORY COMMITTEE FOR AERONAUTICS
1512 H STREET, N. W.
WASHINGTON 25, D. C.

CLASSIFICATION CHANGED TO
UNCLASSIFIED DATE 8-18-
AUTHORITY J.W.CROWLEY
CHANGE # 2350 W.H.L.

CLASSIFIED DOCUMENT

This document contains classified information affecting the National Defense of the United States within the meaning of the Espionage Act, USC 50:31 and 32. Its transmission or the revelation of its contents in any manner to an unauthorized person is prohibited by law. Information so classified may be imparted only to persons in the military and naval services of the United States, appropriate civilian officers and employees of the Federal Government who have a legitimate interest therein, and to United States citizens of known loyalty and discretion who of necessity must be informed thereof.

NATIONAL ADVISORY COMMITTEE FOR AERONAUTICS
WASHINGTON
July 13, 1947

CONFIDENTIAL

NATIONAL ADVISORY COMMITTEE FOR AERONAUTICS

RESEARCH MEMORANDUM

FLIGHT TESTS TO DETERMINE THE EFFECT OF TAPER ON THE ZERO-LIFT DRAG OF WINGS AT LOW SUPERSONIC SPEEDS

By Sidney R. Alexander and Robert L. Nelson

SUMMARY

Results are presented of tests conducted at the Pilotless Aircraft Research Test Station at Wallops Island, Va. to determine the effect of taper on the zero-lift drag of wings of constant exposed aspect ratio at low supersonic speeds. At a constant leading-edge sweep of 45° no orderly variation of drag coefficient with taper ratio occurs, the variation being dependent upon the Mach number. Maximum thickness, leading-edge, and trailing-edge sweep are all important in determining the drag coefficient of a tapered wing.

A comparison is made between the results of theoretical drag calculations of tapered wings and applicable experimental values derived herein.

INTRODUCTION

The advantages of wings of tapered plan forms over straight wings, from structural considerations, have resulted in a general preference for tapered wings in airplane design. In order to obtain information concerning the drag at zero lift of these wings in the transonic and low supersonic speed range, tests have been conducted at the Langley Pilotless Aircraft Research Division Test Station at Wallops Island, Va. of wings having taper ratios from 0 to 1 mounted on rocket-propelled test bodies. Also included are similar data for untapered wings obtained in a previous investigation. The results are presented as curves of total drag coefficient and wing drag coefficient against Mach number. A comparison is made between these results and some theoretical calculations of the drag coefficients of wings of similar plan form.

SYMBOLS

c_t	tip chord measured in free-stream direction, inches
c_r	root chord at wing-fuselage juncture, inches
$\frac{c_t}{c_r}$	taper ratio
l	distance from nose of body to leading edge of root chord, inches
b	total wing span measured from tip to tip normal to body center line, inches
A_{exp}	exposed wing aspect ratio $\left(b_{exp}^2/S_{exp}\right)$
b_{exp}	exposed wing span (not including portion enclosed by body) measured normal to body center line, inches
S_{exp}	exposed area of wing, square feet
$\Lambda_{L.E.}$	angle of sweepback of leading edge, degrees
Λ_m	angle of sweepback of line of maximum thickness, degrees
β	vertex angle formed by extending leading and trailing edges, degrees
W	weight of test vehicle after propellant has been expended, pounds
m	mass, slugs $\left(\frac{W}{g}\right)$
g	acceleration of gravity, 32.2 feet per second per second
D	drag along flight path, pounds
M	Mach number $\left(\frac{V}{c}\right)$
V	velocity of test vehicle, feet per second
c	sonic velocity, feet per second
a	absolute acceleration along flight path, feet per second per second
t	time, seconds

C_{D_T} total drag coefficient of test vehicle based on exposed wing area

C_{D_W} wing drag coefficient based on exposed wing area

CONFIGURATIONS AND TESTS

Configurations.- The basic body used for this general investigation was of all wooden construction, 5 inches in diameter and about 5 feet long. It consisted of a sharp nose of nearly circular-arc profile having a fineness ratio equal to 3.5 to which a hollow cylindrical afterbody was attached. Four stabilizing fins were equally spaced around the rear of the body which had a slight boat tail. These fins were flat surfaces tapered in plan form with rounded leading edges swept back 45° and square trailing edges. The wings which were indexed 45° to the fins were fabricated of laminated spruce and built integral with the center section.

All the test vehicles were propelled by 3.25-inch-diameter Mk. 7 aircraft rocket motors enclosed within the hollow fuselages. At a preignition temperature of 69° F, the rocket motor provides about 2200 pounds of thrust for approximately 0.87 second.

Four different tapered wing plan forms of equal exposed area (1.389 sq ft) and aspect ratio (2.15) were investigated. The principal dimensions of the vehicles tested, together with those for comparable configurations of reference 1, are shown in figure 1. Three of these had a leading-edge sweepback angle of 45° and taper ratios of 0.38, 0.713, and 0, respectively, with the NACA 65-009 airfoil sections taken in the free-stream direction. Photographs of these test vehicles are shown as figure 2. The wing plan form of the fourth test vehicle, shown as figure 3, had a taper ratio of 0 with the NACA 65-006 airfoil sections taken in the free-stream direction. While the test airfoil differed slightly from the NACA 65-006 section, it is felt that the error induced is very small and does not affect the validity of the results. For this fourth plan form, the line bisecting the tip angle β was sweptback 45°. Occasionally this latter configuration will herein be referred to as the arrowhead plan-form wing. The wings were mounted on the body at zero incidence with the mean quarter-chord point at the design center of gravity of the fuselage (station 34.5) and had neither twist nor dihedral. With the exception of the $c_t/c_r = 0.38$ arrangement, two successful flights of each configuration were obtained and the results averaged in the evaluation of the data.

Tests.- The test vehicles were launched at an angle of 75° to the horizontal. Because of the large elevation angle and the short duration of burning of the rocket motor, the trajectories of the vehicles during their coasting flights (after the propellant was expended) were very nearly straight lines. The model flight velocities were measured with a CW Doppler radar set (AN/TPS-5) and for the $c_t/c_r = 0.38$ configuration a Doppler velocimeter located near the point of launching. The Doppler velocimeter is shown in figure 4. These units consist essentially of two parabolic reflectors each with an antenna, one to transmit continuous-wave radio signals of known frequency and wave length along a conical beam and the other to receive them after they are reflected off the moving vehicle. The transmitted and received signals are then "beat" together, and the resultant frequency, which is a function of the velocity of the vehicle, is recorded photographically. The flight velocities are then ascertained from these film records.

The values of temperature and static pressure used in calculating drag coefficients and Mach number were obtained from radiosonde observations made at the time of firing.

The average test Reynolds numbers based on the mean wing chord $\left(\frac{c_t + c_r}{2}\right)$ are given in the following table for $M = 1.2$.

Wing plan form	Taper ratio	Reynolds number
1	1	6.66×10^6
2	0	6.7
3	0.38	6.55
4	0.713	6.53
5	0	6.59
6	1	6.52

REDUCTION OF DATA

The variation of velocity with flight time for two identical configurations with wings of arrowhead plan form is presented in figure 5. The difference in the respective velocities of the two models may be attributed to small differences in model weight and rocket motor performance. The amount of scatter of the experimental points of each curve can be considered negligible. The maximum velocity reached by this configuration was 1490 feet per second. The parts of the respective velocity curves during which coasting flight was attained (after the end of burning) were graphically

differentiated to obtain the deceleration $-a$. The product of the deceleration and the known mass of the test vehicle gave the forward-acting inertia force. This product was equated to the sum of the drag and the known weight of the body; thus $\frac{W}{g}a = d + W$. The values of the drag thus obtained are presented in figure 6 for the models with the arrowhead plan-form wings. As there was some difference in the atmospheric conditions under which these models were fired, the drag curves were reduced to standard sea-level density. The discrepancies between the two curves are a maximum near $M = 1.0$ and are in the order of ± 3 percent, or within the predicted probable accuracy of ± 7 pounds of drag obtained from statistical studies of previous test results conducted by the Langley Aircraft Loads Division.

The total drag coefficients for the models investigated were calculated from the relationship $C_{D_T} = \frac{2W(a - g)}{g\rho V^2 S}$. These values are presented in figure 7. A single curve has been faired through the calculated points for both models of a given configuration. Examination of these curves reveals the scatter of the calculated points from the faired curve is greatest in the Mach number range below 1.0, which is in keeping with the inherent limitations of the testing technique as described in reference 2.

RESULTS AND DISCUSSION

The various faired drag curves are plotted on the same coordinate axes in figure 8(a). For comparison, similar curves for test vehicles with untapered wings having 0° and 45° sweepback angles, and $A_{exp} = 2.15$ (reference 1) are included as well as the drag-coefficient curve for a wingless body. Corresponding curves of wing drag coefficient derived by taking the difference between the C_{D_T} curves of the winged and wingless test vehicles are presented in figure 8(b). These values include any interference effects between the wing and fuselage which may vary for different wing-fuselage combinations.

Plan forms 2, 3, and 4 show the effect of tapering a family of wings having a leading-edge sweep of 45° and exposed aspect ratio of 2.15. Examination of the drag-coefficient curves for these plan forms in figure 8 reveals that no orderly variation of drag coefficient with taper ratio occurs. However, if the variation of other parameters which are affected by the method of tapering is considered, the change in C_D does not take place in an unpredictable manner.

Several investigators (references 3 to 5) have found that when the Mach wave becomes parallel to the leading edge, line of maximum thickness, and trailing edge, drag rises take place. These drag rises should be apparent in the drag-coefficient curve, and in addition should offer a partial explanation of the effects of wing taper on drag.

The fact that the drag-coefficient curve for plan form 2 (0 taper ratio) lies between the curves for the wings of 0.38 and 0.713 taper ratio is an example of the effect of parameters other than leading-edge sweep and taper on the drag. The drag-coefficient curve for wing 2 is very similar to that for any rectangular wing (plan form 1); that is, the curve shows a decrease in drag coefficient with Mach number above $M = 1.1$. Since the line of maximum thickness is very nearly unswept, a drag rise between $M = 1.0$ and 1.2 would be expected. From examination of the curves for plan forms 2 and 4, it is evident that wing 2 has gone through a critical drag rise (maximum at about $M = 1.1$); that is, it has a higher drag coefficient than wing 4 which has gone through no theoretically critical Mach number between $M = 1.0$ and 1.2. (Critical Mach number is the Mach number for which the Mach line is parallel to the leading edge, line of maximum thickness or trailing edge.) The drag resulting from the swept leading edge should reach a maximum at about $M = 1.4$ and thus should be relatively small in this range of Mach numbers. For this reason, the drag-coefficient curve for plan form 2 is similar in shape to the curve for a rectangular wing.

Wing plan form 3 (0.38 taper ratio) has a higher drag coefficient than wing 2 for all Mach numbers investigated. The hump in the curve between $M = 1.0$ and 1.1 may be due to critical trailing-edge sweep and a finite tip chord (for which the wing-tip drag will not be zero at low Mach numbers). It is interesting to note that such a hump is also evident in the drag-coefficient curve for the wingless body which has fins similar in plan form to wing 3. Increasing the Mach number for wing 3 does not reduce the drag coefficient as it did for plan form 2 since the maximum-thickness sweep has become critical at $M = 1.2$. Wing plan form 4 (0.713 taper ratio) has a lower drag-coefficient curve than the wings of 0 and 0.38 taper ratio and is similar in shape to the curve for plan form 6. This would be expected since neither leading-edge nor maximum-thickness sweep are critical. It appears that no drag rise takes place when the trailing-edge sweep becomes critical (at about $M = 1.2$).

Plan forms 1 and 2 show the effect of tapering a rectangular wing about its 50-percent chord line. The large decrease in drag coefficient is due to leading-edge and trailing-edge sweep.

Plan forms 5 and 6 show the effect of fully tapering a constant-chord sweptback wing about its 50-percent chord line. The drag-coefficient curve for wing 5 lies very close to the curve for wing 6, the difference in drag being within the experimental order of accuracy. The trailing-edge sweep of wing 5 is critical at $M = 1.1$. However, as in the case of plan form 4, no large drag rise is evident. This fact may indicate that the trailing edge has a large influence on the drag coefficient only at small angles of trailing-edge sweep. Since no other sweep parameters are critical in this range of Mach numbers, the curves are similar in shape. As indicated previously, wing 5 does not have a true NACA 65-006 airfoil section in the free-stream direction. However this airfoil corresponds closely to that of plan form 6 in the free-stream direction. It is felt that the effect of airfoil section is small and does not affect the validity of the results.

A theoretical curve of drag coefficient plotted against taper ratio for a family of isolated wings having a leading-edge sweepback angle of 45° and aspect ratio of 2.15 is presented in figure 9 for a Mach number of 1.15. The values for this curve were determined from the equations of reference 5 which are valid for taper ratios between 0.37 and 1.0 for the above conditions. Also indicated on the figure are experimental values from data contained herein. The basic relationships are set up for wings of symmetrical diamond profile and give values of wave drag coefficient only. Consequently, an average value of friction drag coefficient of 0.006 has been added to the original calculation. The agreement between theoretical and experimental values is good, considering that the theoretical results are for a different profile and do not take into account interference effects between the wing and fuselage.

CONCLUDING REMARKS

The zero-lift drag characteristics of several tapered wings of equal exposed area and aspect ratio as determined by flight tests of rocket-propelled test vehicles at low supersonic speeds have been presented. For the range of Mach numbers and wing plan forms investigated, the test results lead to the following conclusions:

1. At a constant leading-edge sweepback of 45° no orderly variation of drag coefficient with taper ratio occurs, the variation being dependent upon the Mach number.

2. Maximum thickness, leading-edge, and trailing-edge sweep are all important in determining the drag coefficient of a tapered wing.

Langley Memorial Aeronautical Laboratory
National Advisory Committee for Aeronautics
Langley Field, Va.

REFERENCES

1. Tucker, Warren A., and Nelson, Robert L.: Drag Characteristics of Rectangular and Swept-Back NACA 65-009 Airfoils Having Various Aspect Ratios as Determined by Flight Tests at Supersonic Speeds. NACA RM No. L7C05, 1947.

2. Alexander, Sidney R.: Drag Measurements of a Swept-Back Wing Having Inverse Taper as Determined by Flight Tests at Supersonic Speeds. NACA RM No. L6L30, 1946.

3. Harmon, Sidney M., and Swanson, Margaret D.: Calculations of the Supersonic Wave Drag of Nonlifting Wings with Arbitrary Sweepback and Aspect Ratio. Wings Swept behind the Mach Lines. NACA RM No. L6K29, 1946.

4. Puckett, Allen E.: Supersonic Wave Drag of Thin Airfoils. Jour. Aero. Sci., vol. 13, no. 9, Sept. 1946, pp. 475-484.

5. Margolis, Kenneth: Supersonic Wave Drag of Sweptback Tapered Wings at Zero Lift. NACA RM No. L7E23a, 1947.

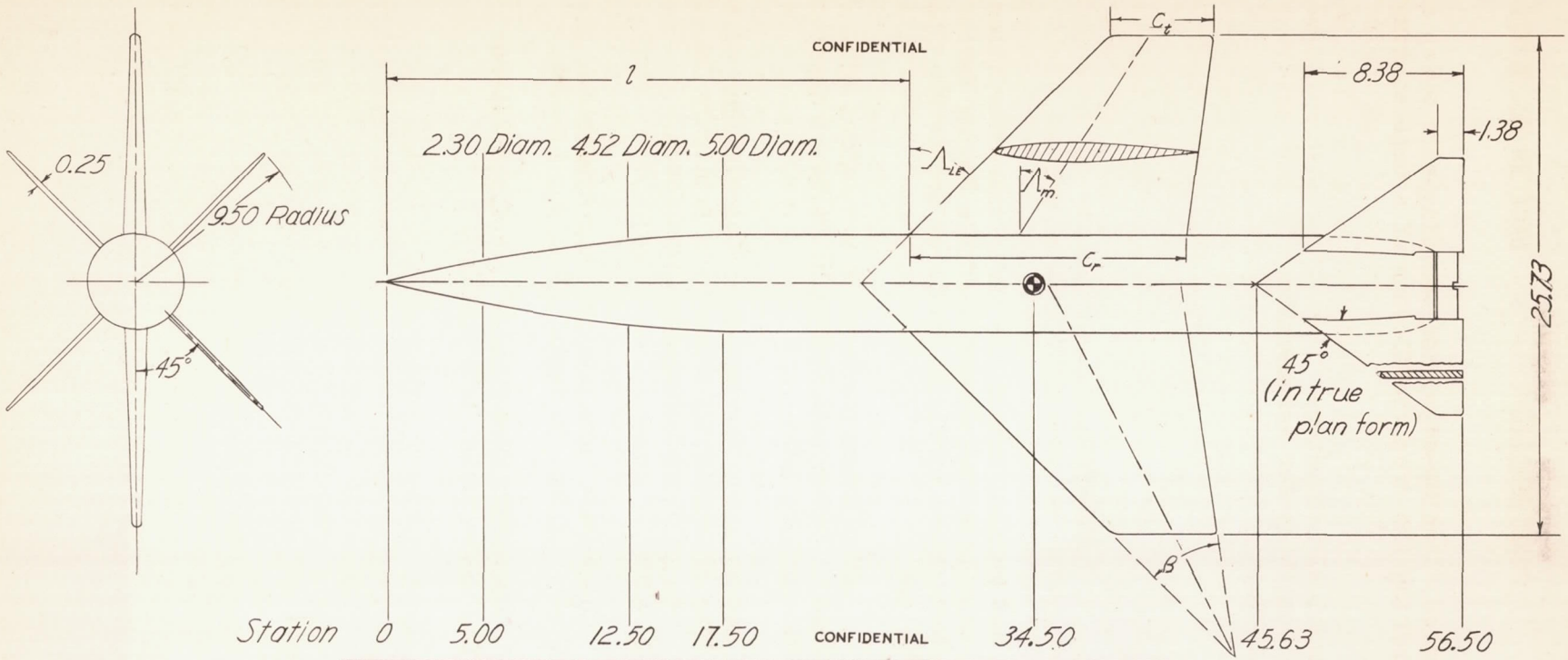

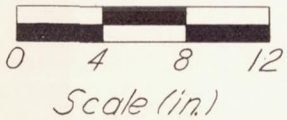

Wing plan form	c_t/c_r	$\Lambda_{L.E}$ (deg)	Λ_m (deg)	c_r (in.)	c_t (in.)	Airfoil Section	l
1	1	0	0	9.65	9.65	NACA 65-009 taken parallel to free stream direction	34.59
2	0	45	10.08	19.294	0		27.84
3	0.38	45	33.66	14.053	5.343		27.51
4	0.713	45	41.25	11.261	8.030		27.17
5	0	66.5	53.75	19.294	0	NACA 65-006 in free stream direction	23.07
6	1	45	45	9.73	9.73		28.26

NATIONAL ADVISORY COMMITTEE FOR AERONAUTICS

Figure 1.- Typical arrangement of test vehicle indicating wing plan forms investigated. Wing area (exposed), 200 sq in; aspect ratio (exposed), 2.15; fin area (4 fins exposed), 136.5 sq in.

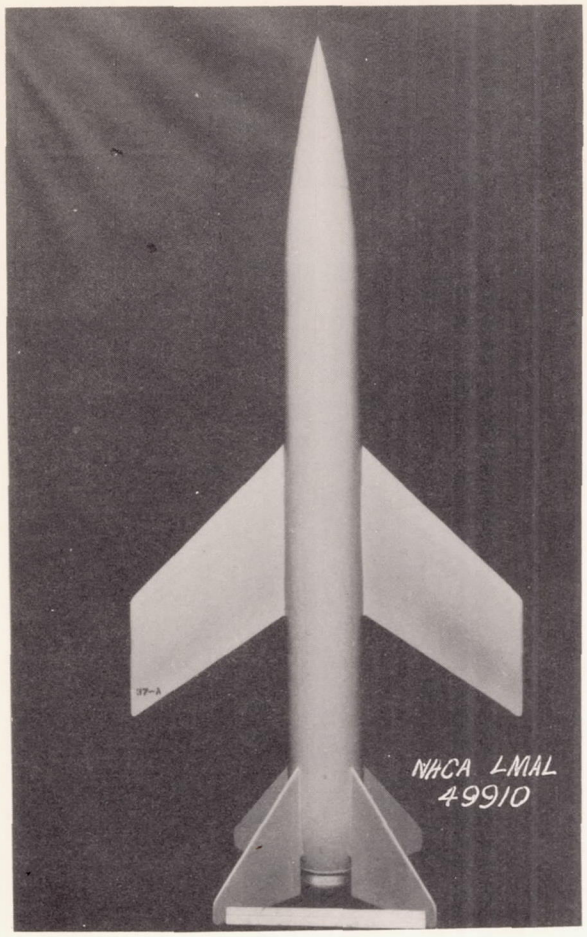

(a) $\frac{c_t}{c_r} = 0.713.$

Figure 2.- Test vehicles showing wing plan forms investigated. $A_{exp} = 2.15$; $S_{exp} = 200$ sq in.; $\Lambda_{L.E.} = 45^{\circ}$.

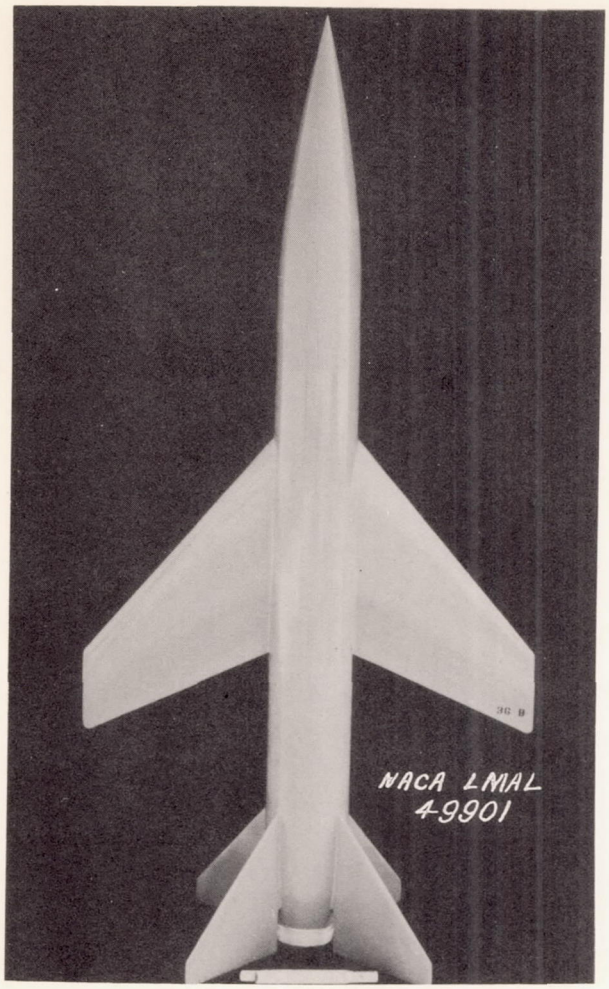

(b) $\frac{c_t}{c_r} = 0.38.$

Figure 2.- Continued.

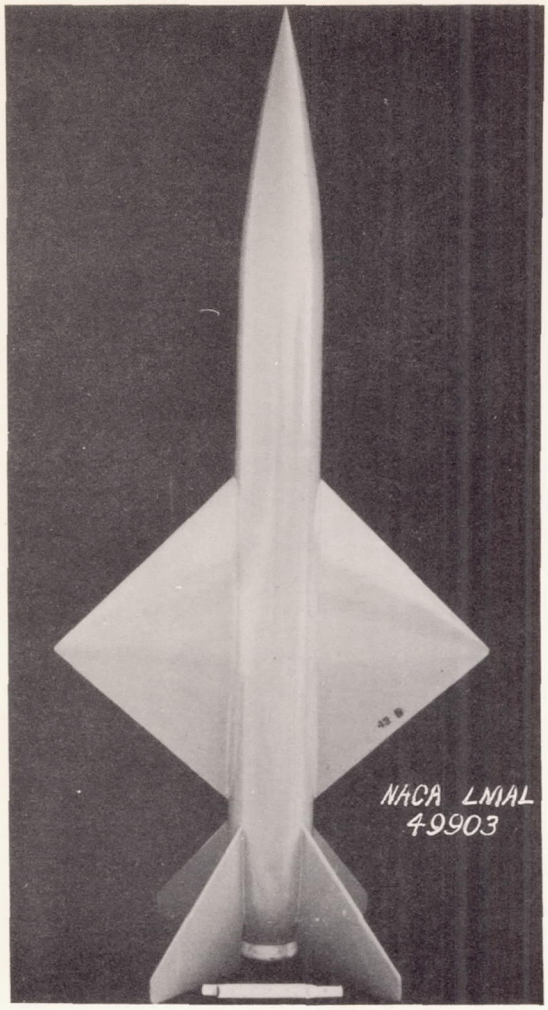

(c) $\frac{c_t}{c_r} = 0.$

Figure 2.- Concluded.

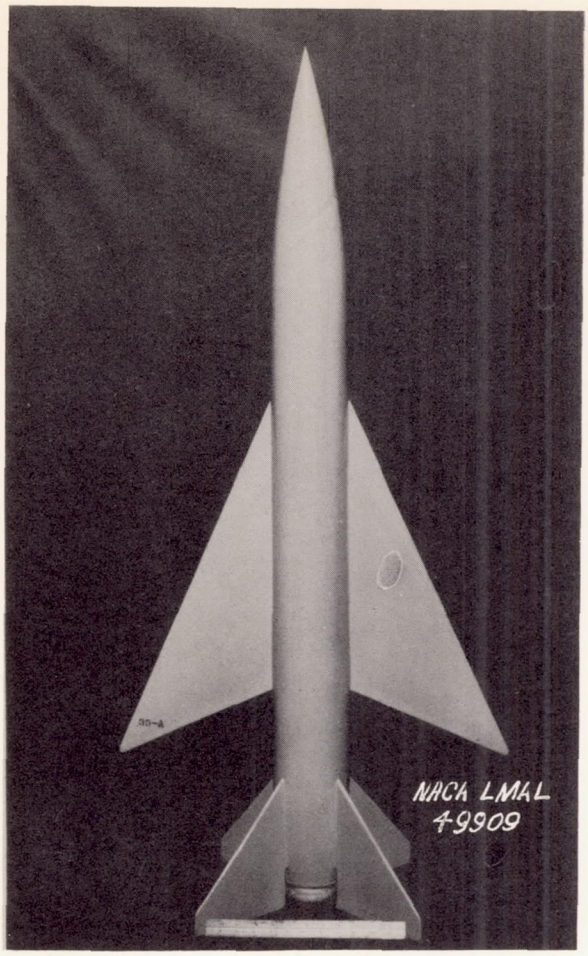

Figure 3.- The test vehicle with wing of arrowhead plan form. $\frac{c_t}{c_r} = 0$; $A_{exp} = 2.15$; $S_{exp} = 200$ sq in.; $\Lambda_{L.E.} = 66.5^{\circ}$.

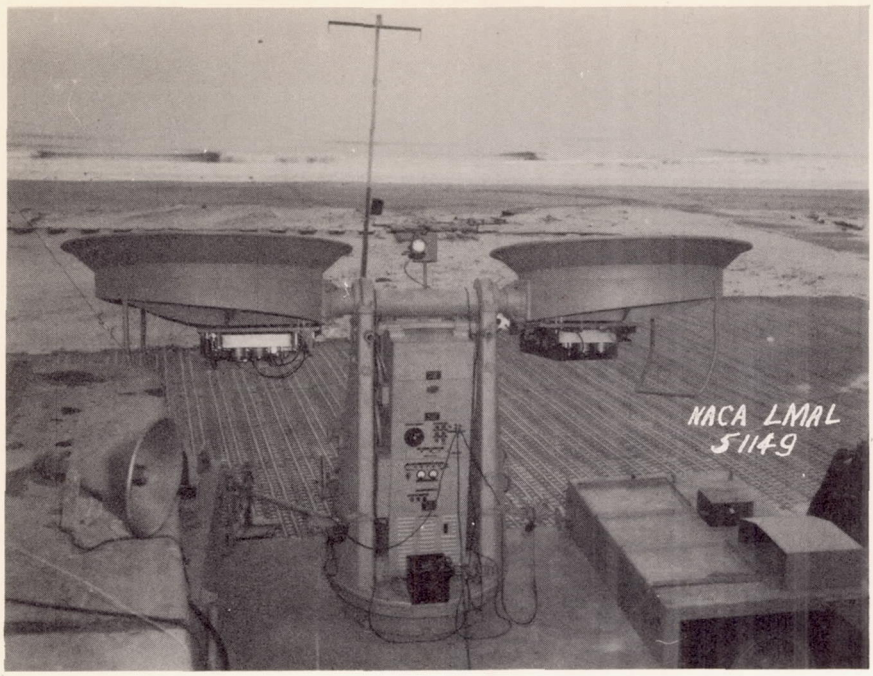

(a) Rear view.

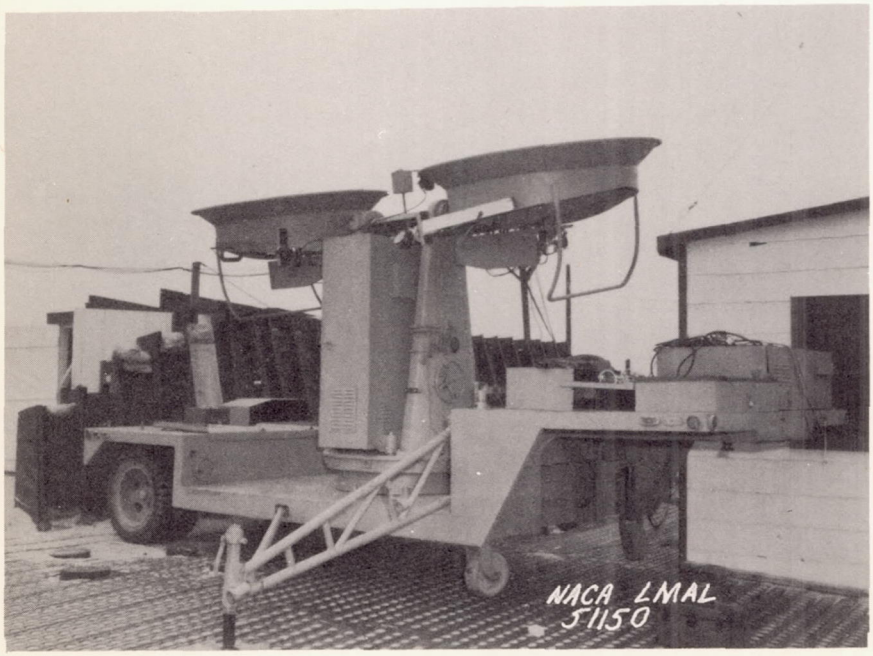

(b) Three-quarter front view. CONFIDENTIAL

Figure 4.- General views of Doppler velocimeter.

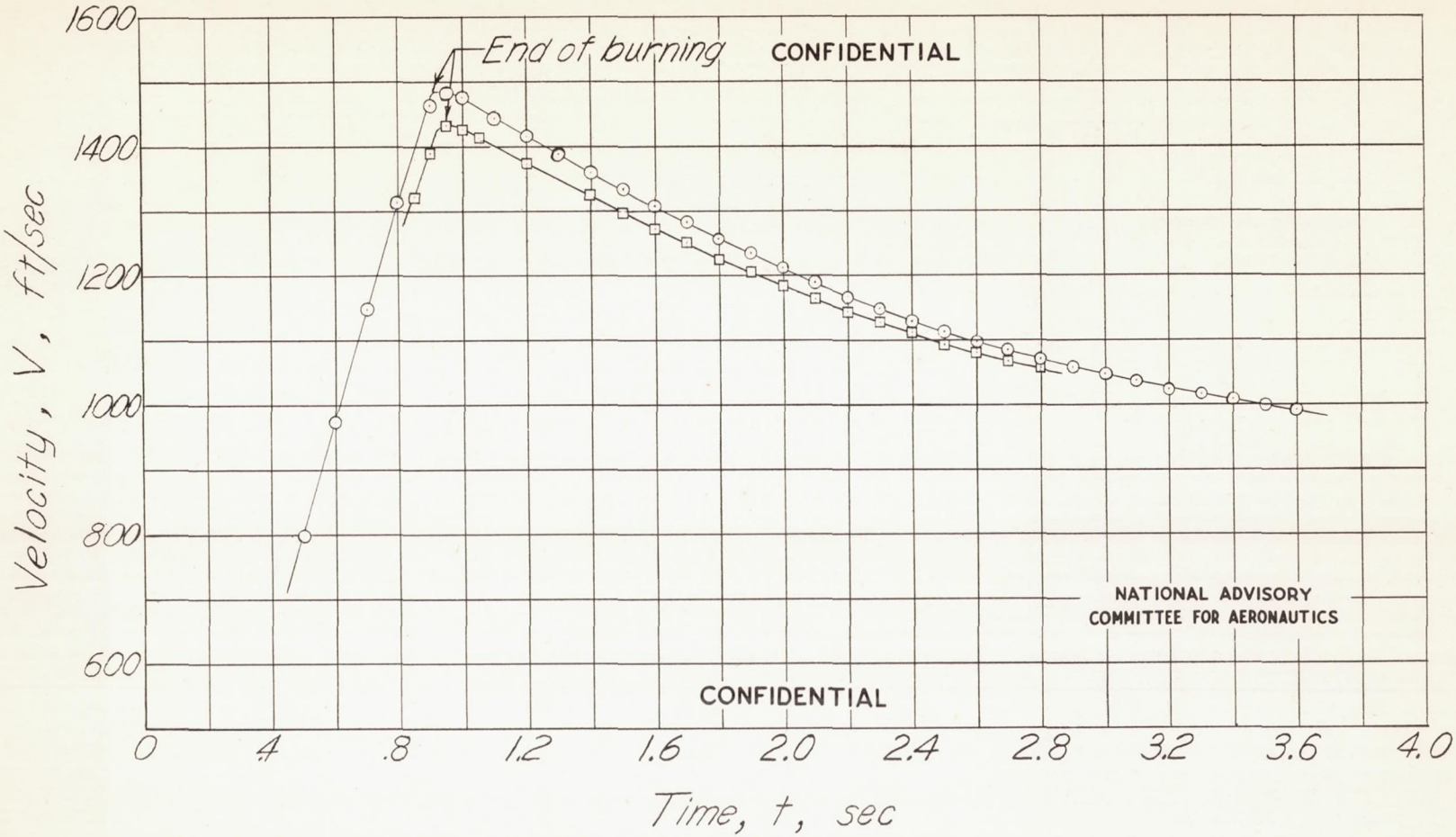

Figure 5 .- Velocity-time curves for two identical test vehicles with wings of arrowhead plan form.

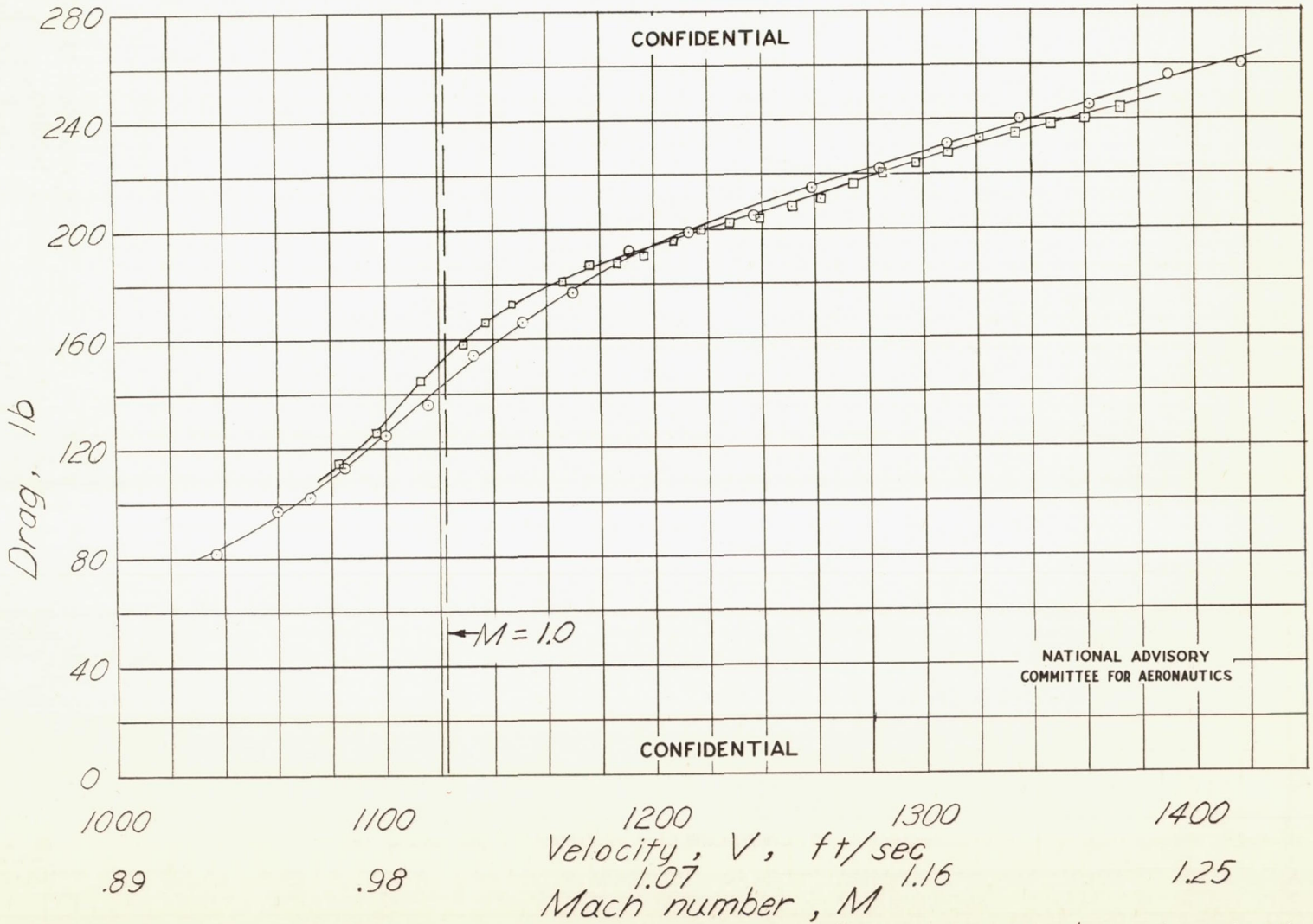

Figure 6.- Comparative drag measurements of two identical test vehicles with wings of arrowhead plan form.

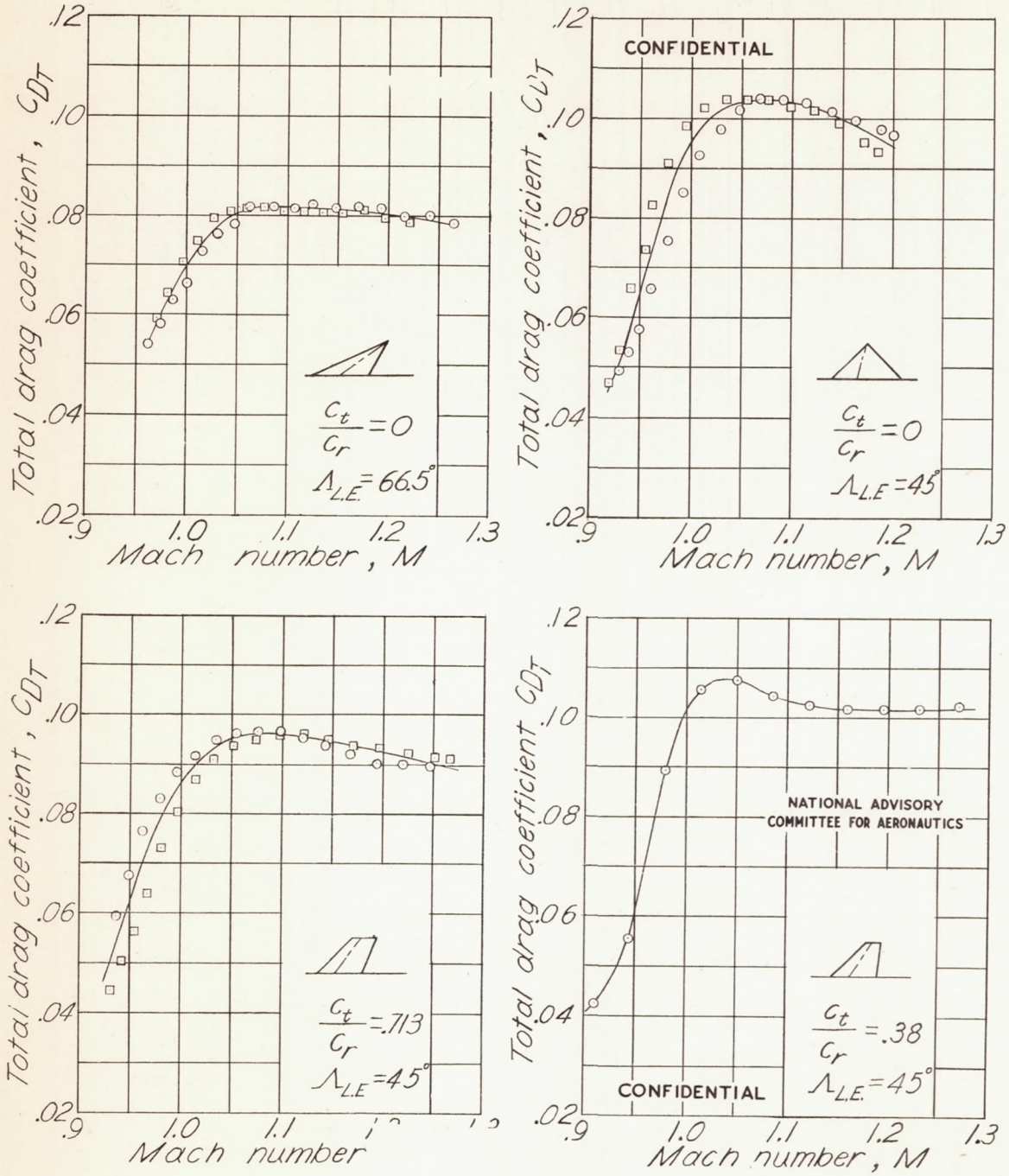

Figure 7.- Variation of total drag coefficient with Mach number showing original test data for all models of each configuration tested. $A_{exp} = 2.15$.

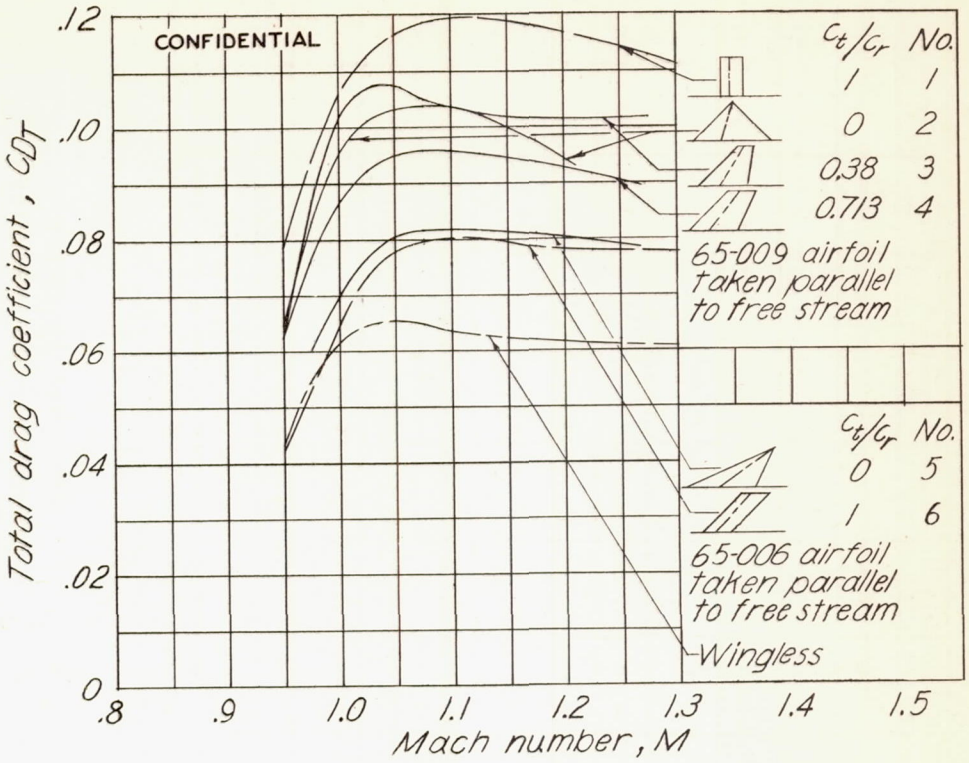

(a) Total drag coefficient.

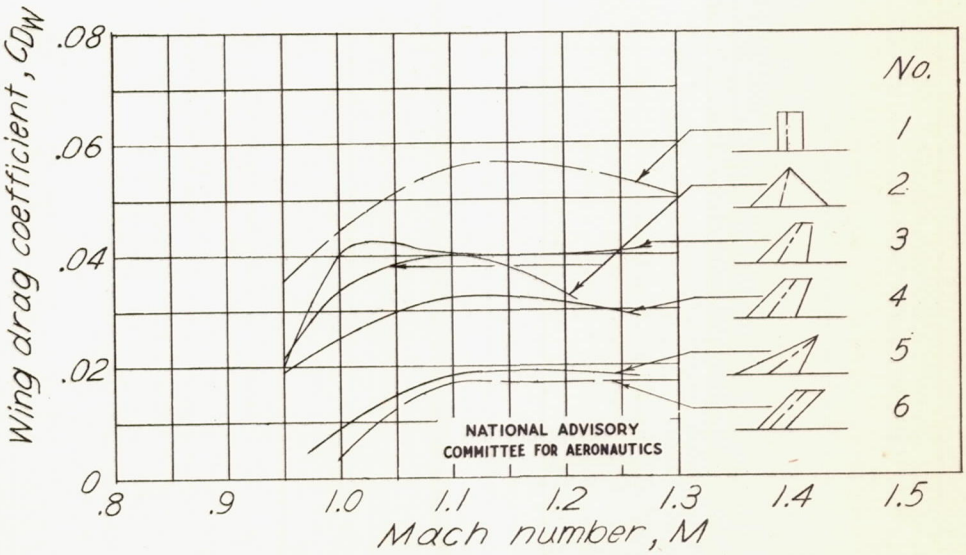

(b) Wing drag coefficient.

Figure 8.- Effect of taper on total drag coefficient and wing drag coefficient. $A_{exp.} = 2.15$.

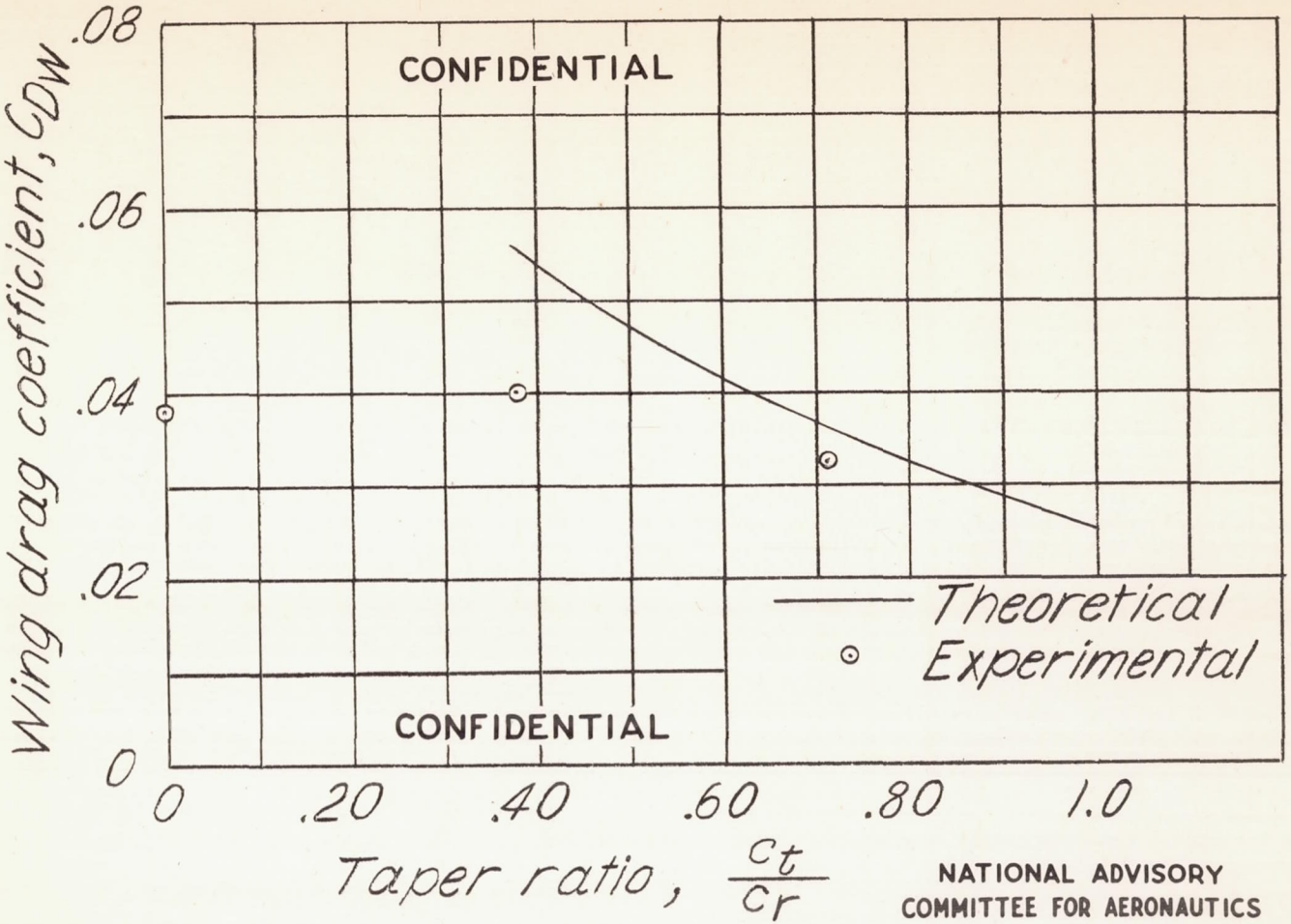

Figure 9.- Comparison of experimental and theoretical variation of wing drag coefficient with taper ratio. $A_{exp.} = 2.15$; $\Lambda_{L.E.} = 45°$; $M = 1.15$.